

# OVERVIEW OF ESS BEAM DIAGNOSTICS

A. Jansson, C. Böhme, B. Cheymol, H. Hassanzadegan, M. Jarosz, T. Shea, L. Tchelidze, European Spallation Source ESS AB, Lund, Sweden

## Abstract

The European Spallation Source (ESS) will use a 2.5GeV superconducting proton linac with a 5MW average beam power to produce the world's most powerful neutron source. The project, sited in the south of Sweden, is approaching the end of the pre-construction phase, and is expected to enter the construction phase in 2013. This paper gives an overview of the ESS accelerator and the planned beam diagnostics systems, as well as the associated challenges.

## THE ESS ACCELERATOR

The European Spallation Source (ESS) is a 5MW linac-based neutron source, which will be built in Lund, Sweden. It has a pulse repetition rate of 14Hz, a nominal beam current of 50mA and a pulse length of 2.86ms. Acceleration is provided by a warm RFQ and DTL operating at 352MHz, followed by superconducting spoke cavities (also at 352MHz), and two types of elliptical cavities operating at 704MHz. The overall length of the linac is about 400m, followed by an additional 160m of upgrade space and transfer line.

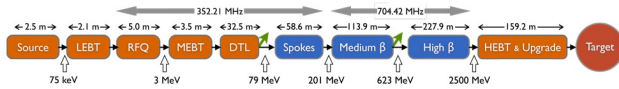


Figure 1: ESS linac layout overview.

The project is currently in a pre-construction phase. A conceptual design report[1] was recently released, and a Technical Design Report (TDR) along with an updated cost estimate is planned for the beginning of 2013. An overview of the current project status has been presented in recent conference proceedings [2].

## PLANNED DIAGNOSTICS SUITE

The ESS LINAC optics is under configuration control since since 2010, with biannual updates. The discussion below is based on the October 2012 lattice release. This lattice is also the one that used in the Technical Design Report.

### Warm Linac

The LEBT (see Fig. 2) consists of two solenoids for focussing (each equipped with a steering magnet) plus a chopper to trim the beginning and end of the ion source pulse. In the LEBT, the source emittance will be measured using a slit and one of two sets of SEM grids. The SEM grids also allow measurement of the beam profile and position directly. The beam current will be measured at the entry and exit using beam current transformers. An insertable Faraday cup also allow for beam current measurement and double as a temporary

beam stop. An inclined viewport to determine ion species fraction by observing Doppler shifted luminescence light is also foreseen.

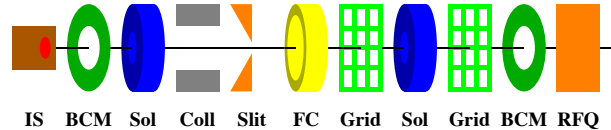


Figure 2: LEBT diagnostics layout.

The MEBT[3] will have 10 quadrupoles, three buncher cavities and a fast chopper (see Fig. 3). Here, the transverse emittance from the RFQ will be measured with a slit and grid system, employing a slit design similar to LINAC4. In addition, a set of 4 wire scanners will be used to measure the beam profile. Two of these are co-located with viewports for non-invasive profile measurement based on luminescence, and two are co-located with transverse halo measurement stations. Six BPMs will be used for TOF and position measurement, and two BCT will be inserted at the beginning and at the end of the line for intensity and transmission measurement. A movable Faraday cup allow for beam current measurement and double as a tune-up beam dump. Longitudinal beam profile measurement will be performed with a Beam Shape Monitor (BSM).

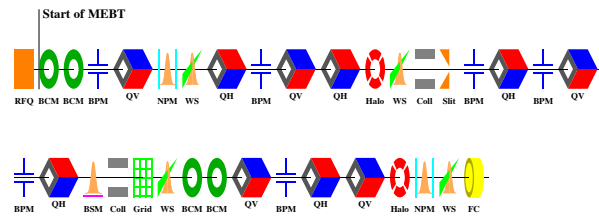


Figure 3: MEBT diagnostics layout.

The Drift Tube Linac (DTL) consists of four tanks (see Fig. 4). It employs a permanent magnet FODO lattice leaving empty drift tubes for diagnostics. The first tank will have two BPMs, and the following tanks one BPM each. The SNS-like inter-tank regions will each house a wire scanner, a Faraday cup, and viewports for non-invasive profile monitoring. In addition, each tank will have a BCT incorporated in the end wall.

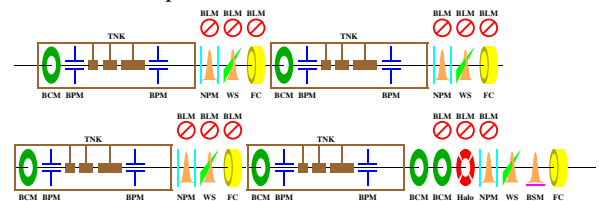


Figure 4: DTL diagnostics layout.

### Cold Linac and Upgrade Space

The cold linac consists of three main sections, using spoke cavities, medium beta elliptical cavities and high beta elliptical cavities, respectively. The entire cold linac uses a doublet lattice with one cryomodule per cell in the spoke and medium beta section, and two cryomodules per cell in the high beta section. There is dedicated space for beam diagnostics between the warm magnets in the doublets. Here, it is foreseen to have one dual plane position pick-up attached to each magnet and three loss monitors placed before, between and after the quadrupoles. An additional BLM will be placed between adjacent cryomodules in the high beta section. The layout of the spoke section is shown in Fig. 5.

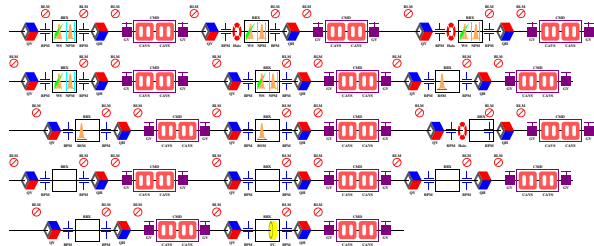


Figure 5: Spoke cavity section diagnostics layout. The other sections are similar.

The cell length changes significantly between three main sections, causing a change in the focussing. To ensure proper matching, it is foreseen to equip the beginning of each major section with four transverse profile monitors and four longitudinal profile. Tungsten wire scanners are the reference transverse profile devices. They will be co-located with a system using a non-invasive technique, that can be used for full intensity. A beam current monitor at the beginning of each section is also foreseen.

The cold linac is followed by a 100m section of HEBT which doubles as upgrade space[4]. It has the same doublet optics as the high beta elliptical, but without cryomodules. Consequently, instrumentation here is similar to the high beta section.

### Beam on Target and Dump

Towards the end of the HEBT there is a switching magnet that can send the beam either to the target (A2T line) of the tune-up dump. The target spur has an achromatic vertical bend to go from the linac tunnel level below grade to the target, which is above the ground level. Before the beam hits the target, it is expanded and its distribution flattened using octupoles. To verify the beam distribution and position in these magnets, each is equipped with a wire scanner and a viewport for non-invasive profile. Most quadrupoles are equipped with a BPM and a BLM for position and loss measurement (see Fig. 6). There is also a BCT to measure transmission and monitor total beam on target.

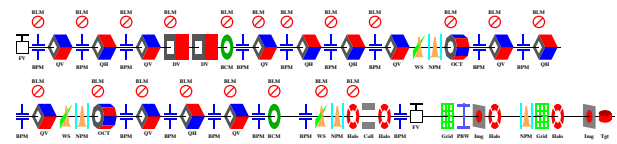


Figure 6: Target transfer line diagnostics layout.

It is critical that the beam delivered to the target has the right distribution. A local beam density that is too high may lead to target damage. Therefore, a target beam distribution monitoring system is needed. The same is true for the proton beam window, which separates the accelerator vacuum from the target helium atmosphere. Due to the importance of protecting the target, redundant methods are being pursued. A similar system will also be used to monitor the beam size on the tune-up beam dump.

### “DAY ONE” DIAGNOSTICS

Some diagnostics system will mainly become important when ramping up to production power. However, certain systems need to function from “day one”, for initial commissioning. These include BLMs, BCMs, and BPMs. Some invasive “day one” devices, such as Faraday Cups, can only be used with low power beam due to thermal load.

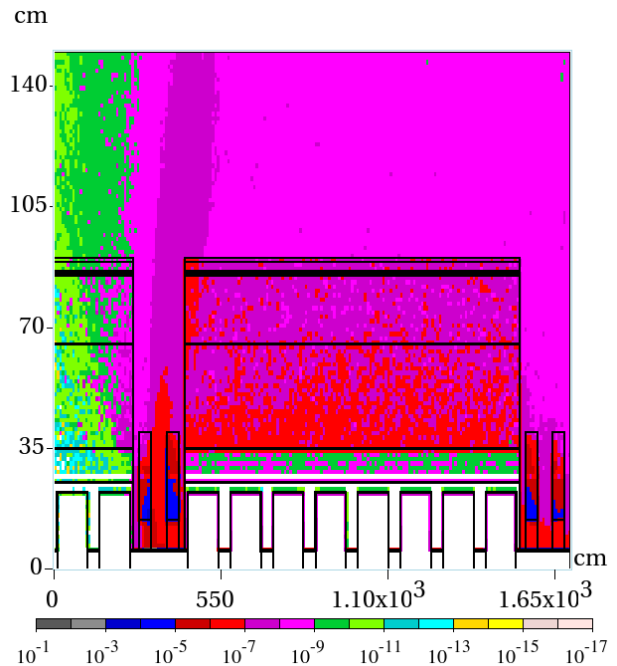


Figure 7: Simulated loss distribution from beam loss on the aperture in the first doublet quadrupole in the high beta section.

### Beam Loss

The beam loss monitoring (BLM) is arguably the most important diagnostic system of the ESS linac. It has the dual purpose of keeping the machine safe from beam-induced damage and avoiding excessive machine activation by providing critical input to the machine protection system. Thus, the system must be designed for

complete coverage of possible loss scenarios. In addition, as the BLM system will be a major tool for beam tune-up, it should also be designed in a way that enables it to pinpoint the loss location as precisely as possible. The optimal location of detectors is being determined by simulations (see Fig. 7).

Ionization chambers (ICs) will be the main beam loss detector. SNS or CERN LHC type detectors may be used, and are currently being evaluated. Fast PMT-based detectors and neutron detectors will also be used in some locations.

The required sensitivity for the ICs is set by the desire to limit machine activation. The chosen criteria is that the BLM system should be able to detect a continuous loss leading to beam pipe activation of 1% of the hands-on maintenance limit (or about 0.01W/m). The response time, on the other hand, is determined by the ability to detect large fast losses. Simulations show that if the entire beam is lost in a single spot, it can melt steel in a matter of a few us in the warm linac (a few 10s of us in the cold linac). Thus, the requirement for the BLMs system is to detect such a losses within 2us for the warm linac (10us for the cold linac). SNS or LHC style ICs may be used, possibly with some modification.

At low energies, ionization chambers are not very effective to detect beam loss due to the self shielding from the RFQ and DTL tanks. Here differential current measurement will be used as a complementary beam loss detection mechanism.

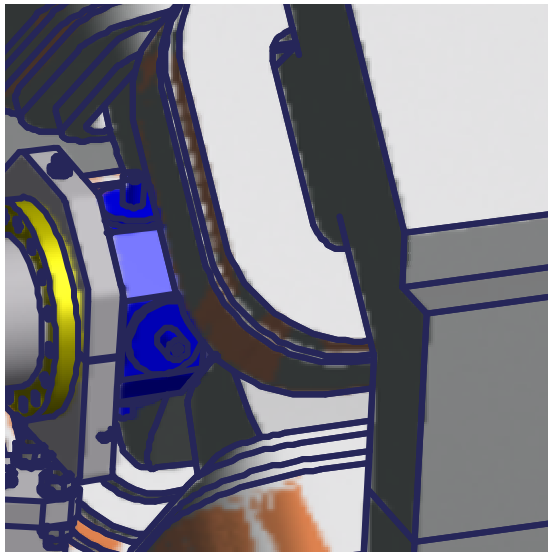


Figure 8: Detail showing button BPM located in the shadow of the quadrupole coil, requiring no extra longitudinal space.

### Beam Position

The BPM system will measure the beam position, the beam phase with respect to the RF reference, as well as an approximate beam current.

Button electrodes will be used, except in the DTL drift tubes where special shorted striplines are foreseen. As far as possible, BPM sensors will be physically attached to

each quadrupole, since the goal of beam steering normally is to center the beam in the quadrupoles. Again, the DTL is the primary exception, since the permanent magnet quadrupoles take most of the available space in a drift tube, forcing the BPM to reside in its own drift tube. In the A2T line, beam should be centered in the octupoles, so BPMs will be located on or near these strong, non-linear magnets. In the cold linac, BPMs can be installed in the shadow of the quadrupole coils, requiring no extra longitudinal space (see Fig. 8).

The BPM electronics will consist of a fast analog front-end, where the BPM signals will be received by sensitive analog electronics, level adjusted and conditioned. Following this, a digital section will digitize the signals and processed them in an FPGA. Processing will be narrow band, and the processing frequency will be different from the local cavity frequency (704MHz up to the spoke section, and 352MHz from the elliptical cavity sections onwards). Narrow band processing requires some additional correction at the low energy end of the linac, since the sensitivity for a given frequency is not only given by the geometry of the pick-up, but also is a function of the relativistic beta. The BPM electronics should have a large enough dynamic range and a good signal-to-noise ratio so that they give useful results even for beam currents down to 5 mA and pulse lengths down to 5 us respectively. A particular challenge is that during tune up of the cold linac, beam may need to be transported very long distances to reach a beam dump, and in the process the beam debunches, leading to a significant drop in the harmonic content of the signal.

### Emittance

Two emittance measurements will be permanently installed in the warm linac and will be based on a slit and grid system.

In the LEBT, preliminary estimations of the thermal load show that TZM, tungsten and graphite are well suited for the slit material. Between the two solenoids, the beam size is relatively large and the slit can handle the full beam pulse.

Two SEM grids will be used to reconstruct the angular distribution of the beam. Carbon wires are the primary choice for the monitor due to the good thermal properties of this material, the grid pitch will has to determined in function of the beam parameters. The complete mechanical design is on going, and thermo mechanical analysis will provide the operating envelope of the system.

The MBT slit and grid system required a more complicated design. At 3 MeV, the thermal load is an issue and the slit cannot operate during the production mode. Based on LINAC4 design [5], graphite is the best solution for slit material. To lower the thermal load, the energy deposition is spread on a larger surface by tilting the slit with respect to the beam axis. Figure 9 shows the maximum temperature on the slit for 3 angles (45°, 30° and 15°) in function of the beam pulse length.

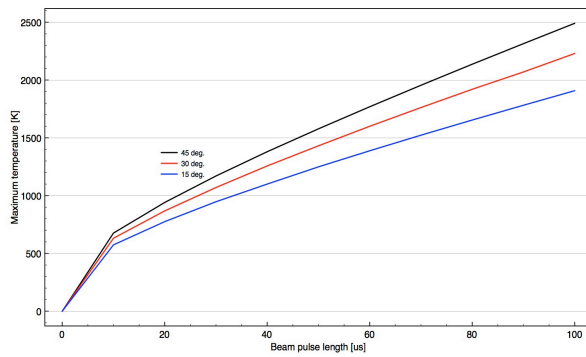


Figure 9: Maximum temperature on a graphite slit for different slit angle in function of the beam pulse length.

The mechanical limits of graphite are around 1600 K, the estimation of the temperature shows that the slit cannot handle a 100  $\mu\text{s}$  beam pulse. In order to preserve the slit integrity, the pulse length has to be reduced to 50  $\mu\text{s}$ , in this case, an angle of 30° is enough to keep the thermal load below the limits of the graphite.

The other concern about the MEBT emittance meter is the resolution of the profile monitor. Due to the short drift space, the pitch of the SEM grid shall be 100  $\mu\text{m}$  for the vertical plane and 300  $\mu\text{m}$  for the horizontal plane in order to reconstruct the beamlet profile with enough accuracy. These pitches cannot be achieved, other solutions are considered like wire scanner or layer of carbon and metal foil.

### Faraday Cups

During the commissioning and the tuning phase of the ESS linac, insertable Faraday cups will measure current while isolating the downstream accelerator components from beam. Due to thermal load, the Faraday cups can only be inserted into the beam line during dedicated beam modes. Except in the LEBT Faraday cup, the beam must be in the diagnostics pulse mode.

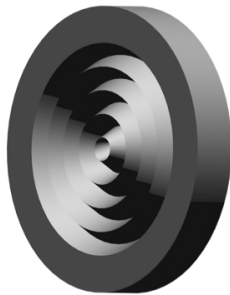


Figure 10: LEBT graphite Faraday collector shape.

The LEBT Faraday cup will be installed in between the two solenoids, where the beam sizes are relatively large. Despite the low energy of the beam, the power deposition per unit volume is high due to the short penetration depth. In order to increase power handling, graphite with a special shape will be used (see Fig. 10). With these design features, the LEBT Faraday cup will be the only one capable of handling pulses much longer than diagnostic pulse. Preliminary simulations show that the FC might be

used in production mode with external cooling. At low energy, the secondary emission yield is large, and a bias voltage is foreseen to suppress the secondary emission.

The challenge of the MEBT FC is to keep the thermal load below the mechanical limits of the FC, due to the small beam sizes and the large stopping power of 3 MeV protons. This system will also feature a wide bandwidth channel, capable of monitoring MEBT chopper performance.

The design of the DTL Faraday cups is based on the SNS design and includes an energy degrader in front of a graphite collector. The energy degrader absorbs the low energy particles that have fallen out of the accelerating bucket. The thickness and the material of depends on the expected beam energy. The degrader also absorbs part of the beam that is at nominal energy, and the scattering will increase the beam sizes at the collector and reduce the thermal load. The peak energy density is reduced by 10% in case of graphite energy degrader and up to 30% with copper.

Monte Carlo simulations show also that a non-negligible amount of particles are created in the energy degrader. The amount of nuclear interaction increases with the beam energy and the particles produced can perturb the measurement. In the worst case, 3 % of the beam charge is lost in the energy degrader, so that a correction must be applied to the data in order to meet the accuracy requirements.

### Wire Scanners

Wire scanners will be used only with a special short diagnostics pulse. In the warm linac section, the calculations show that a carbon wire will survive if the beam pulse is reduced to 100  $\mu\text{s}$  and 1 Hz repetition rate, although thermionic emission can be an issue.

Recent studies performed at GANIL show that carbon wires are incompatible with superconductive cavities, so tungsten wires are foreseen for wire scanners in the cold linac. Due to the lower stopping power at high energy, these wires will survive if they are used with a short diagnostic pulse.

At low energies, the secondary emission current on the wires will be used to determine the profile. Above 200 MeV, the profile will be reconstructed by sampling the shower created by the wire with a segmented scintillator; the type and the geometry of the detector are still under studies. However, initial studies show that good linearity can be obtained even in the short space available by summing multiple detectors to avoid geometric effects (see Fig. 11).

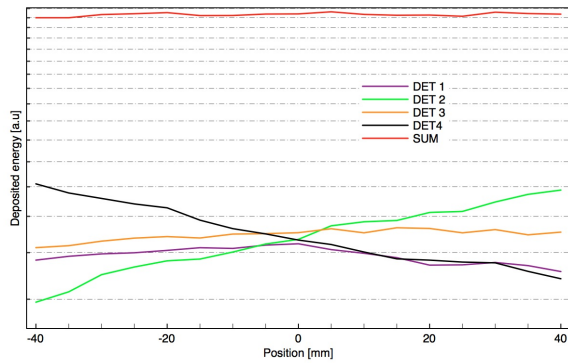


Figure 11: Simulated energy deposition in four scintillators placed around the beam pipe approximately 40cm downstream of a wire scanner, as a function of wire position.

## MEASUREMENT CHALLENGES

### Target Imaging

To monitor the power density on the target and proton beam window, an imaging system similar to the one developed at SNS is foreseen [6]. The baseline solution employs luminescent coatings on beam-intercepting surfaces. A dedicated instrumentation module within the target monolith (see Fig. 12) will contain optics to view the target face and the downstream side of the proton beam window.

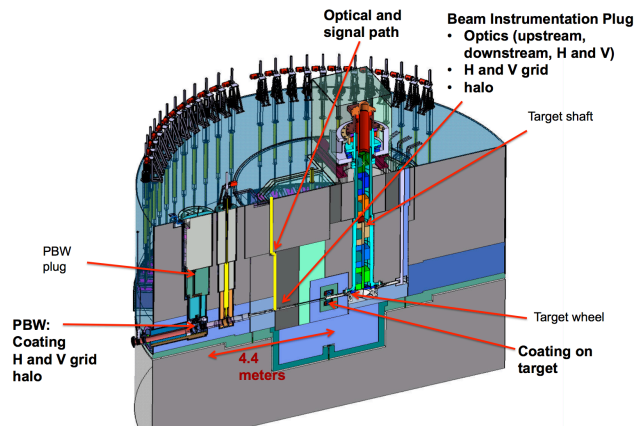


Figure 12: Target monolith schematic showing the location of the target wheel, proton beam window and the diagnostics plug with optical and signal paths.

The proton beam window presents a particular development challenge, since a thermal spray coating of the type used at SNS would add significantly to the window's mass. The proton beam window is also where the beam density will be the highest (see Fig. 13). Due to the importance of monitoring beam properties in this region, additional solutions are also being explored, including gas fluorescence, wire grids, and optical transition radiation.

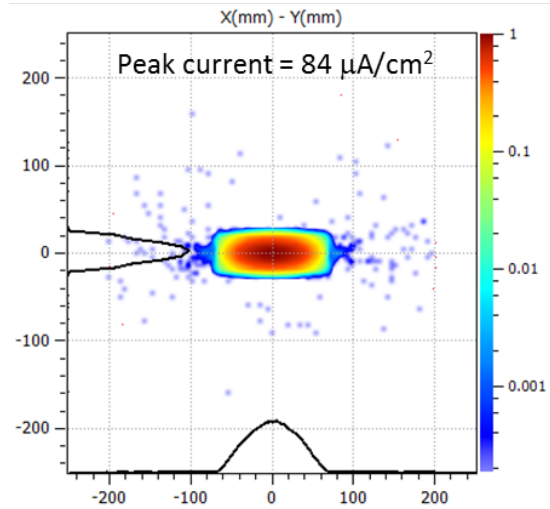


Figure 13: Beam distribution on the proton beam window. (Figure courtesy of Aarhus University)

### Longitudinal Bunch Shape

Bunches in the ESS LINAC are very short (see Fig 8), and therefore options to measure the bunch length are limited. The low velocity and relatively wide aperture mean that any device based on the wall current or field at the aperture have an intrinsic resolution much larger than the bunch length. Such a detector is based on measuring secondary electrons from a wire placed in the tail of the beam distribution. Since the process of electron emission does not have a significant delay, very good time resolution can in principle be achieved. Variants of such a monitor without a physical wire have been developed at GSI and ANL, and these are interesting options for ESS. A particle beam profile scanner (see next section) could also be modified in order to measure the bunch length. The BSMs could also in principle be used as wire scanners, but the baseline design separates these functions to allow optimization of each device for their respective applications.

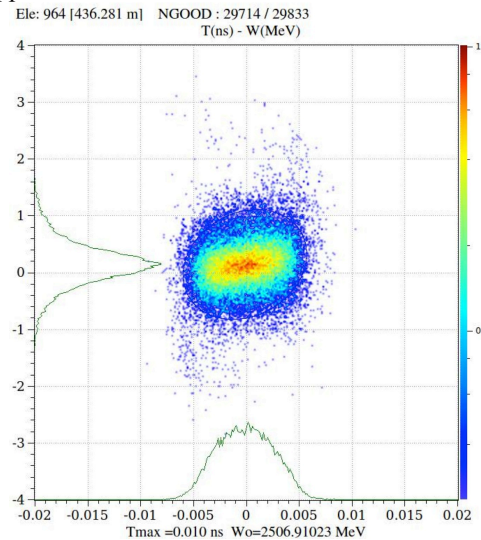


Figure 14: Longitudinal beam distribution at the end of the linac (Figure courtesy of R. Miyamoto, ESS).

### Non-invasive Beam Profile

Since wire scanners can only be used for special low power beams, non-invasive methods for measuring beam profiles are being investigated in parallel. Some methods in investigation are residual gas ionization (IPM) [7], luminescence (LPM) [8] and an electron scanning method [9]. These methods could allow measurements of the beam profile during neutron production. However, they are often not considered as exact as wire scanners and may have limited resolution at low beam powers, so invasive devices will be retained for cross calibration even where the non-invasive devices are installed.

Tests to establish the luminescence yield for vacuum conditions similar to the ESS linac have been initiated in collaboration with SNS. A sketch of how such a monitor could be integrated in the space available between doublet quadrupoles is shown in Fig. 15.

The emitted light due to the interaction between the beam and the residual gas can also be used to measure the relative fraction of ions species coming out of the ion source. With a digital camera installed in the focal plane of a monochromator with a few tens of degree angle with respect to the beam propagation axis, the Doppler shift observation of the  $H_{\alpha}$  hydrogen Balmer series allows isolating the fluorescence of each ions species of the beam. The ratio of the different ions is proportional to the light intensity [10].

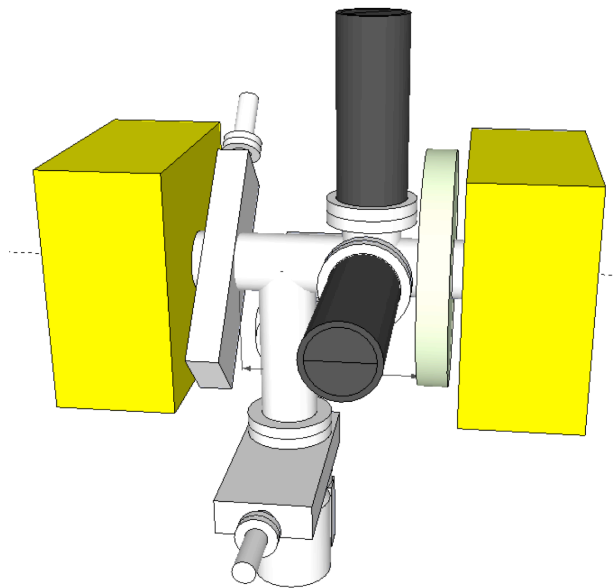


Figure 15: Sketch showing possible integration of a shower mode wire scanner (scintillator shown in green) with a dual plane luminescence monitor and pumpout port between doublet magnets in the High Beta upgrade section.

### Halo

In order to keep the losses at a small level, the beam transverse halo will be measured at several locations along the ESS linac and cleaned with several collimators. In the warm linac, the halo measurement can be performed with wire scanners equipped with high gain and high dynamic range electronics. Similarly, the charge deposition in the MEBT collimators can be also measured. In the cold linac, this method cannot be employed and different options are under investigation, such as the use of a wire scanner equipped with a Cherenkov fiber, or the use of diamond detectors.

The radiation hardness of the material is an issue and the life time of the detector remains to be estimated. The drawback of these two methods is that they cannot measure the profile of the beam core. In the UHB line, a wire scanner equipped with a particle detector telescope will be used in counting mode to measure beam core and halo with the same device.

Within the target monolith, thermocouples surrounding the physical aperture will be used to measure position of the beam envelope.

### SUMMARY

This paper has outlined diagnostics suite for the ESS accelerator, and some particular challenges related to it. An overview of the various types of instruments in different parts of the LINAC is given in Table 1.

### REFERENCES

- [1] ESS Conceptual Design Report
- [2] H. Danared et al, Design of the ESS Accelerator, IPAC12, New Orleans, LA
- [3] I. Bustinduy, Medium Energy Beam Transport Design Update For ESS, IPAC12, New Orleans, LA
- [4] A I Sander-Holm et al, The Layout of the High Energy Beam Transport for the European Spallation Source, IPAC12, New Orleans
- [5] B. Cheymol et al., "Design of the Emittance Meter for the 3 and 12 MeV LINAC4 H- Beam", IPAC'10, Kyoto, Japan
- [6] T.J. Shea et al., "Installation and initial operation of an on-line target imaging system for SNS", Proceedings of 19th meeting on International Collaboration of Advanced Neutron Sources (ICANS XIX), Grindelwald, Switzerland, PSI-Proceedings 10-01 / ISSN-Nr. 1019-6447, March 2010.
- [7] C. Böhme et al, TUPB12, DIPAC09
- [8] C. Böhme et al, TUPB10, DIPAC09
- [9] W. Blokland et al, TUOA03, DIPAC09
- [10] F. Senee et al., "Diagnostics for High Power Ions Beams with Coherent Optic Fiber for IFMIF-EVEDA Injector", DIPAC' 09, Basel, Switzerland

Table 1: Summary of Planned Instrumentation Systems

Section	BL M	BCM	BPM	Slit (H+V)	Grids (H+V )	FC	WS	Non- Invasive Profile	Optical imaging	Halo	BSM
LEBT		2		1	2	1					
MEBT		4	6	1	1	1	4	2		2	1
DTL	12	6	8			4	4	4		1	1
Spoke	42		28				5	5		3	3
Low Beta Elliptical	48	2	32				4	4		4	4
High Beta Elliptical	60	1	30				4	4		4	4
HEBT (to switch)	22	2	14				4	4		2	2
Target Line	20	2	16		2		3	3	2	4	
Dump Line	10	2	8		1		1	1	1	1	
Total	214	21	142	2	5	6	29	28	3	21	15